AUTOMATED HASP GLASS SEARCH USING THE ELECTRON MICROPROBE.

C. T. Adcock, M. N. Spilde, and J. J. Papike, Institute of Meteoritics, Department of Earth and Planetary Sciences, University of New Mexico, Albuquerque, New Mexico 87131, USA. E-mail: yoyodine@unm.edu

Summary: Using an automated electron microprobe analysis technique, we have located and measured, high-aluminum, silica-poor (HASP) glasses in a suite of lunar samples previously analyzed by Vaniman in 1990 [4]. The automated electron microprobe (EMP) technique determines the location of possible lunar HASP glasses in thin section using criteria based on size, backscattered electron intensity and weight percent of Si and Al by energy dispersive spectroscopy (EDS). Once located, the possible HASP glasses are revisited and analyzed by wavelength dispersive spectroscopy (WDS) to determine if the glasses meet the criteria to be classified as HASP glasses. The automated package located HASP glasses both previously identified and unidentified in five Apollo 14 thin sections (14076,5 / 14252,5 / 14263,25 / 14282,5 / 14160,148). HASP beads identified by this process were then analyzed by Secondary Ion Mass Spectrometry [1]. The automated technique allows for thin sections to be scanned for specific features quickly and without constant supervision.

Methods: We used a JEOL 733 Superprobe EMP equipped with an Oxford LINK eXL II analyzer. The user interface includes an image analysis package called Featurescan. We configured Featurescan to detect and measure HASP-like glass beads. Features in a field of view that meet both size and backscattered electron intensity criteria are then analyzed by EDS to determine if they meet the general chemical criteria to be HASP glasses. If a feature meets all of the criteria, the position of the feature in the field of view as well as the position of the field of view on the sample are written to a file and the features are revisited later and analyzed with more accurate WDS analysis. The ability of the Oxford interface and Featurescan to create grids of fields of view and drive the EMP stage allows analyses to be carried over the area of the entire thin section in a period of a few hours.

Discussion and Results: The uniqueness of HASP glasses was first realized during research on the Apollo 16 samples [2]. Most other lunar glasses can be explained through impacts sampling primary crystalline rocks, the mixing of products from previous events, or as volcanic products. HASP glasses, on the other hand, seem to require differential vaporization for formation. HASP glasses are generally classified by having an Al_2O_3 content of greater than 16 wt% and an SiO_2 content of less than 40 wt%[4]. However, these classifications are not strictly used [3], and the term HASP is used to represent any lunar glass in which the genetic implications are Al enrichment due to Si volatilization from impact. HASP glasses seem to show general Al_2O_3:SiO_2 trends, depending on the Apollo sampling site [4] (see Fig. 1). The more HASP glasses identified and analyzed in a sample, the more tightly these HASP trends can be constrained.

The automated package we developed not only located HASP glasses found in a prior study by Vaniman [4], but an additional 18 HASP glasses (more than double the previous amount). WDS analyses of these HASP glasses are presented in Table 1. All of the data presented in the table were collected in this study; however, the table also contains cross references to beads previously found by Vaniman in his 1990 study [4]. Figure 1 shows the trends established from the analyses. These analyses fall mainly on the previously established [4] Apollo 14 trend with the exception of analyses from sample 14076,5. This deviation in 14076,5 is consistent with data collected by Vaniman [4]. The HASP tend line for the Apollo 16 site is included in the diagram for reference and is based on previously collected data [2].

Conclusions: The automated EMP package located both previously known and unknown HASP glasses in lunar thin sections expanding the available data on HASP glasses and improving the understanding of HASP Al_2O_3:SiO_2 trends. The ability of the automation package to quickly identify HASP-like features without supervision greatly improves the efficiency where these very rare features must first be located in a sample before analyses can be performed. There is no reason the developed package cannot be used to find other types of glasses or features in a variety of thin section samples.

Acknowledgments: EMP analyses were performed at the UNM Institute of Meteoritics Microprobe Lab. This research was funded by NASA grant NAGW-3347 and the Institute of Meteoritics. Catalog of previously identified glasses supplied by D. T. Vaniman, Los Alamos, New Mexico.

References: [1] Papike, J.J., et al. this publication. [2] Naney, M.T. et al., (1976) Proc. Lunar Sci. Conf. 7th 155-184. [3] Norris, J.A. et al., (1993) Lunar and Planetary Science XXIV, 1093-1094. [4] Vaniman, D.T., (1990) Proc. Lunar Sci. Conf. 20th, 209-217.

Table 1. Elemental concentrations by weight % of Apollo 14 HASP Glasses.
* Bead numbers in third column refer to beads previously located by Vaniman [4].

Section #	Bead #	Vaniman Bead#*	SiO_2 wt%	Al_2O_3 wt%	TiO_2 wt%	MgO wt%	FeO wt%	CaO wt%	Na_2O wt%	K_2O wt%	Total wt%
14076,5	I-01	CL-07	35.26	42.74	0.13	0.65	0.63	21.08	0.01	0.02	100.5
14076,5	I-02	CL-13	27.13	46.28	0.10	0.23	0.03	25.98	0.20	0.01	100.0
14076,5	I-03	YE-14	33.39	39.51	0.26	2.30	0.27	24.78	0.05	0.00	100.5
14076,5	I-04	CL-18	22.45	53.19	0.08	1.47	0.07	23.16	0.07	0.00	100.5
14076,5	I-05	CL-21	19.52	52.20	0.09	0.18	0.00	28.78	0.02	0.00	100.8
14076,5	I-06	CL-43	27.58	46.31	0.07	0.08	0.02	25.40	0.36	0.00	99.8
14160,148	I-01	none	39.87	18.80	2.06	10.57	13.08	14.09	0.00	0.00	98.5
14160,148	I-04	YE-03	37.65	23.78	2.05	11.65	8.43	15.16	0.00	0.00	98.7
14160,148	I-05	none	36.19	22.51	2.60	13.11	9.54	14.29	0.01	0.00	98.3
14160,148	I-06	YE-06	35.64	22.54	2.44	11.81	10.07	14.50	0.00	0.00	97.0
14252,5	I-01	YE-07	38.53	22.67	2.49	11.47	10.31	14.04	0.01	0.00	99.5
14252,5	I-02	none	40.52	21.87	2.30	10.55	10.51	13.40	0.02	0.00	99.2
14252,5	I-03	none	40.07	22.05	2.23	12.02	9.97	13.51	0.00	0.00	99.9
14252,5	I-04	none	39.16	20.75	2.36	11.36	11.35	13.15	0.01	0.00	98.1
14252,5	I-05	none	39.08	22.44	2.29	12.35	10.00	13.86	0.02	0.00	100.0
14252,5	I-06	none	37.85	22.63	2.37	11.88	10.28	14.08	0.00	0.00	99.1
14252,5	I-07	none	36.34	22.47	2.48	12.94	10.38	14.12	0.00	0.00	98.7
14252,5	I-08	none	38.95	22.21	2.00	11.68	11.07	13.68	0.00	0.00	99.6
14252,5	I-09	none	39.81	25.97	2.28	10.31	5.30	16.43	0.09	0.00	100.2
14252,5	I-10	none	40.19	19.59	1.99	12.72	12.60	12.04	0.00	0.00	99.1
14263,25	I-01	none	38.43	17.89	2.39	12.46	14.91	11.60	0.00	0.00	97.7
14263,25	I-02	none	30.14	23.53	2.63	11.22	15.50	14.24	0.00	0.00	97.3
14263,25	I-03	CL-2	41.62	21.71	2.11	10.70	9.58	12.79	0.01	0.00	98.5
14282,5	I-01	none	41.90	15.59	2.49	9.32	14.49	13.28	0.00	0.00	97.1
14282,5	I-02	none	35.94	21.26	2.39	14.40	9.93	13.95	0.00	0.00	97.9
14282,5	I-03	none	38.22	19.74	1.93	13.59	11.47	12.11	0.02	0.00	97.1
14282,5	I-05	none	35.73	23.03	3.07	9.58	10.33	14.79	0.00	0.00	96.5
14282,5	I-07	none	35.15	22.14	2.21	12.69	11.26	13.79	0.00	0.00	97.2

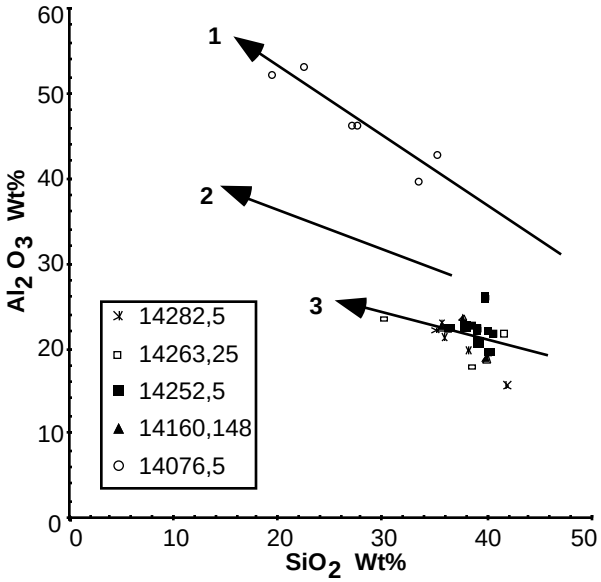

Figure 1. An XY scatter plot of the WDS analyses (Al_2O_3 vs. SiO_2) with trend lines: 1 - sample 14076,5 HASP trend, 2 - Apollo 16 HASP trend, 3 - Apollo 14 HASP trend.